ELSEVIER

Journal of Nuclear Materials 246 (1997) 53–59

journal of nuclear materials

Atomistic modeling of finite-temperature properties of β-SiC. I. Lattice vibrations, heat capacity, and thermal expansion

Lisa J. Porter *, Ju Li, Sidney Yip

Department of Nuclear Engineering, Massachusetts Institute of Technology, Cambridge, MA 02139-4307, USA

Received 11 November 1996; accepted 19 March 1997

Abstract

We present a two-part theoretical study of the thermal properties of crystalline β-SiC based on an empirical interatomic potential developed by Tersoff which emphasizes the bond-order nature of covalent solids. In part I we use this description of interatomic interactions in both lattice dynamical calculations and molecular dynamics simulations with a temperature-scaling procedure to obtain reasonably accurate predictions of the heat capacity and the thermal expansion coefficient. Our results notwithstanding, improvement of the potential to include ionic interactions for the description of vibrational properties, and extension of short-range forces beyond the nearest neighbors, would be quite useful. © 1997 Elsevier Science B.V.

1. Introduction

Silicon carbide is a material which has wide ranging structural [1], electronic [2], and nuclear applications [3] by virtue of its high-temperature strength and mechanical stability, high thermal conductivity, wide band-gap characteristics, and low level of induced radioactivity. Not surprisingly therefore, there is continued interest in developing fundamental theoretical and computational models that are capable of describing the various physical properties of this material. On the other hand, despite the fact that many of these applications involve high temperatures, little attention has been given thus far to our ability to adequately predict the thermal properties of SiC.

The purpose of this work is to present results on the thermodynamic properties of a perfect crystal of polytype 3C (β-SiC) obtained by an atomistic modeling approach. By adopting an interatomic potential model which treats the material as purely covalent, we show that the heat capacity and thermal expansion coefficient are quite well described, whereas the calculated phonon dispersion curves clearly reveal the effects of ignoring electrostatic interactions. In a companion paper, a parallel study of thermal conductivity is reported where, in addition, we have considered the effects of several types of point defects: vacancy, interstitial, and antisite.

In atomistic modeling of materials properties and behavior, the single most important consideration is the description of interatomic interactions, a problem that can be treated at one of three levels. At one extreme, ab initio electronic structure methods [4] provide the most accurate description; however, they are also the most computationally demanding. This approach is at present restricted to simulation systems of about 100 atoms, and is generally considered not yet practical for finite-temperature studies. At the other extreme is the classical potential model [5,6] which, though highly empirical, is computationally the most tractable. At the intermediate level is the tight-binding approximation [7,8] which involves a simplified treatment of the band-structure contribution to the energy; this hybrid method is an attempt to combine the advantage of an electronic-structure description with the computational simplicity of atomistic calculations. For the present study of thermal properties of β-SiC, an empirical potential [9] will be adopted on the grounds that applying either the ab initio or the tight-binding approach would be computationally prohibitive and difficult to justify a priori.

* Corresponding author. 5925 Highdale Circle, Apt. D, Alexandria, VA 22310, USA. Tel.: +1-703 924 2058; e-mail: lporter@ida.org.

[1] See, for example, various papers in Ref. [1].

PII S0022-3115(97)00035-4

The potential model used in this work is a many-body description developed by Tersoff for covalent crystalline solids. Originally applied to tetrahedrally bonded silicon [10], it was later extended to carbon [11], and then to SiC by combining the individual models for Si and C with a Si–C interaction parametrized to give the correct heat of formation [9]. Compared to other empirical potentials proposed for Si, the Tersoff model is noteworthy for its bond-order nature which emphasizes the role of local coordination in determining the strength of a bond between two atoms. Thus, the potential is formulated so that the interaction between a pair of atoms becomes weaker when there are more neighbors surrounding the pair, consistent with the physical behavior known from chemical bonding theory [12]. Applications of the Tersoff model to Si have been summarized and compared with other empirical potentials [13]; more recently, studies of structural transformation [14], melting [15], point defects [16,17], and thermodynamic properties [18] using this potential have been reported.

In contrast to Si for which many empirical potentials have been proposed, few attempts at developing comparable descriptions for SiC have been reported. Besides the Tersoff model, an early potential based on the inclusion of an explicit three-body interaction in a manner similar to the Stillinger–Weber model [19] for Si was suggested by Pearson et al. for use in surface studies [20]. Another approach, based on a modification of the embedded atom method, was recently proposed by Baskes [21]. Thus far, applications reported include studies of tension-induced cleavage [22], point defect structures [23], surfaces [24], thermomechanical properties [25], and pressure-induced amorphization [26]. A comparison of the elastic constants shows that the Tersoff potential is superior to the other two models [25].

We begin by reviewing in Section 2 the Tersoff model from the standpoint of the bond order parameter and the interaction range cutoffs, both aspects having a bearing on the performance of the potential in finite-temperature calculations. In Section 3 the two computational approaches used in this work are described, lattice dynamics and molecular dynamics simulation, along with a procedure relating the simulation temperature and the temperature of the physical system. In Section 4 results are given for a single crystal of β-SiC, first the vibrational properties of the density of states and dispersion curves, and then the heat capacity and thermal expansion. This paper concludes with remarks on how the potential description may be improved for a specific application.

2. Interatomic potential description – The Tersoff model of β-SiC

In the bond-order potential description of Tersoff [9–11,27,28], the interatomic interaction between any two atoms in the lattice consists of a repulsive component and an attractive component,

$$V_{ij} = f_c(r_{ij})\left[A_{ij}e^{-\lambda_{ij}r_{ij}} - B_{ij}e^{-\mu_{ij}r_{ij}}b_{ij}\right]. \tag{2.1}$$

The function $f_c(r_{ij})$ cuts off the interaction beyond an outer distance S and is unity up to an inner distance R; between R and S it varies smoothly. The essential feature of the model is the bond order parameter b_{ij} which is a measure of the strength of the bond between atoms i and j; this quantity depends on the presence of the other atoms in the neighborhood of the interacting pair [9,12]. It has the functional form

$$b_{ij} = \frac{\chi_{ij}}{\left(1+\beta_i^{n_i}\zeta_{ij}^{n_i}\right)^{1/2n_i}}, \tag{2.2a}$$

where

$$\zeta_{ij} = \sum_{k\neq i,j} f_c(r_{ik})\,g(\theta_{ijk}), \tag{2.2b}$$

and the function $g(\theta_{ijk})$ is given by

$$g(\theta_{ijk}) = 1 + \frac{c_i^2}{d_i^2} - \frac{c_i^2}{\left[d_i^2 + (h_i - \cos\theta_{ijk})^2\right]}. \tag{2.2c}$$

One sees that the bond-order parameter depends explicitly on the local environment through the summation in Eq. (2.2b). First, an increase in the number of atoms in the neighborhood (coordination number) will cause the i–j bond to weaken. Second, the separation distance between atom i and an environmental atom k also can affect the bond-order parameter through the cutoff function in Eq. (2.2b). Lastly, the bonding geometry plays a direct role through the function $g(\theta_{ijk})$, which depends on the angle between bond i–j and bond i–k.

The parameter set used in the present work is given in Table 1. Note that the carbon parameters are those given in Ref. [27] (see also the footnote in Ref. [28]). Unlike the other ten parameters, the values for R and S were not optimized; they were simply chosen to lie between the first

Table 1
Parameters used in the Tersoff potential parameter carbon silicon

Parameter	Carbon	Silicon
A (eV)	1.5448×10^3	1.8308×10^3
B (eV)	3.8963×10^2	4.7118×10^2
λ (nm^{-1})	0.34653	0.24799
μ (nm^{-1})	0.23064	0.17322
β	4.1612×10^{-6}	1.1000×10^{-6}
n	0.99054	0.78734
c	1.9981×10^4	1.0039×10^5
d	7.0340	16.217
h	−0.39953	−0.59825
R (nm)	0.18	0.27
S (nm)	0.21	0.30
	$\chi_{Si-C} = 1.0086$	

and second nearest neighbors of the static lattice. Only one property of SiC, the heat of formation, was used to fix the cross-interaction, and that was to determine the parameter χ_{ij}. For all other parameters describing the interaction between Si and C, simple combining rules were applied:

$$\lambda_{ij} = \frac{\lambda_i + \lambda_j}{2}, \tag{2.3a}$$

$$\mu_{ij} = \frac{\mu_i + \mu_j}{2}, \tag{2.3b}$$

$$A_{ij} = \sqrt{A_i A_j}, \tag{2.3c}$$

$$B_{ij} = \sqrt{B_i B_j}, \tag{2.3d}$$

$$R_{ij} = \sqrt{R_i R_j}, \tag{2.3e}$$

and

$$S_{ij} = \sqrt{S_i S_j}. \tag{2.3f}$$

As indicated in Eqs. (2.3), the parameters for the Si–C interaction are based on the values for the individual elements. Thus, the values of R and S for the Si–Si interaction in SiC were taken to be the same as for pure Si, 2.7 Å and 3.0 Å, respectively. In Si the equilibrium bond-length is 2.35 Å and the second-nearest neighbor distance is 3.84 Å, so the values of R and S are reasonable. Using the same values for SiC, however, poses an obvious problem. Because the bond-length of SiC is only 1.86 Å, the distance between Si atoms in SiC is 3.03 Å. Thus, at finite temperature, thermal motion can easily reduce the Si–Si distance to below 3.0 Å. When this occurs the effective coordination number of a Si atom can jump from four to as high as sixteen. Even if the coordination number just increases by one, a significant increase in the energy could result. Not all Si–Si interactions will affect the energy in the same way; those that form small angles with the Si–C bonds will have the greatest effect [25].

Besides the increased amplitude of displacement at elevated temperatures which allows the second-nearest neighbors to interact, another way for these interactions to take place is through an external loading. To avoid this effect, the cutoff distance was made proportional to the lattice parameter [25], so that a uniform contraction of the system under hydrostatic compression would have no influence on the cutoff function. However, for finite temperature simulations at zero pressure, this scaling, if anything, would exacerbate the problem. From the standpoint of ensuring that only nearest neighbor interactions are taken into account during a simulation run, we have found that the simple procedure of excluding the Si–Si interactions regardless of their separation distance gives the best results.

3. Methodology for modeling thermal properties

3.1. Harmonic / quasiharmonic approximation

For a system of N atoms the $3N$ normal modes of the system can be obtained by diagonalizing the force–constant matrix

$$D_{i\alpha j\beta} = \frac{1}{\sqrt{m_i m_j}} \frac{\partial^2 U}{\partial r_{i\alpha} \partial r_{j\beta}}, \tag{3.1}$$

where U is the potential energy of the system, i and j denote the atom number, and α and $\beta = x$, y, and z. The force–constant matrix for the Tersoff potential has been derived analytically. See Ref. [18] for details.

A histogram of the $3N$ modes provides a discrete density of states. In the case of a perfect crystal, one can also determine the continuous density of states by taking advantage of the periodicity of the lattice in reciprocal space. The equations of motion are transformed into an eigenvalue problem

$$\|\mathbf{D} = \omega^2 \mathbf{I}\| = 0, \tag{3.2}$$

where $\mathbf{D}$ is the dynamical matrix, the Fourier transform of the force–constant matrix given in Eq. (3.1). The calculation of the density of states thus consists of generating k-points in the reciprocal space and solving Eq. (3.2) for each k-point.

We have employed two different methods of generating the k-points. In the first method, a uniform grid is laid down in the Brillouin Zone. At each point in the grid, we determine whether an equivalent point has already been listed, using the 48 cubic symmetries. If not, it is added to the list. In the second method, we employ a random sampling technique. We generate a random k-point within a cube of side $2\pi/a$ (where a is the lattice parameter), and then determine whether it is in the first Brillouin Zone. If it is, then it is accepted. While the two methods yield essentially identical results, it turns out that the second method is faster. We present the density of states in Fig. 1a.

Fig. 1b shows the phonon dispersion curves given by the Tersoff potential. (Previous results given in [25] contained an error.) Comparison with experimental data [29–31] indicates that the optical frequencies are overestimated, and the TO and LO modes are degenerate at the Γ point, in contrast to the experimental results. As noted before [25], the problem lies in the fact that the potential describes only covalent bonding whereas β-SiC is known to be 12% ionic. The LA mode is fairly well reproduced, but the TA mode is overestimated, which is a common feature of this potential (see, for example, [18]). A comparison of Fig. 1a and b indicates that the acoustic modes correspond to frequencies at or below about 19 THz, while the optic modes have frequencies exceeding about 27 THz.

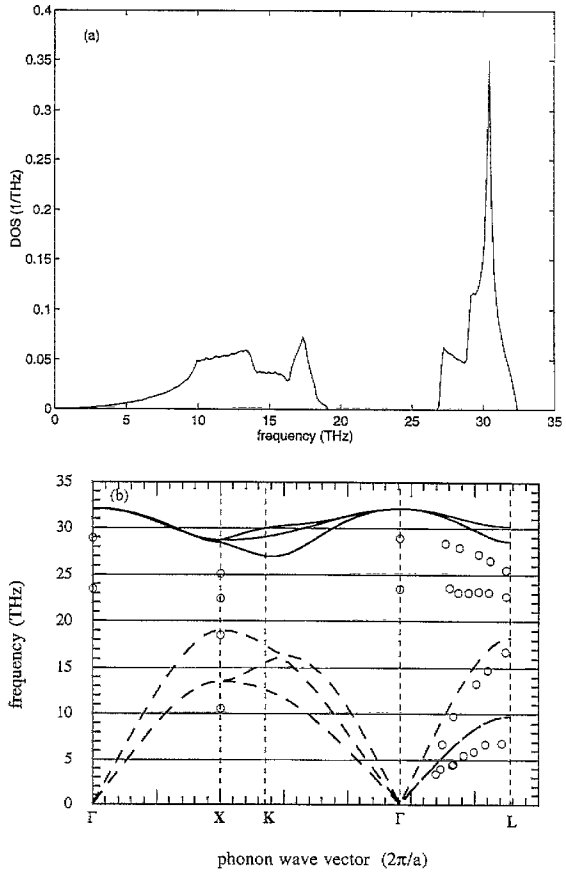

Fig. 1. (a) Vibrational density of states of β-SiC at 0 K obtained from the Tersoff potential, and (b) Phonon dispersion curves of β-SiC at 0 K obtained from the Tersoff potential (optical modes are solid lines, and acoustic modes are dashed lines), and experimental data [29–31] (open circles).

Given the phonon frequencies obtained from Eq. (3.1), one can readily calculate various thermodynamic properties using the harmonic approximation. Thus, the internal energy and the heat capacity are given by

$$E = U_0 + \frac{1}{2}\sum_i \hbar\omega_i + \sum_i \frac{\hbar\omega_i}{\left[\exp(\hbar\omega_i/k_B T) - 1\right]}, \quad (3.3)$$

$$C_V = k_B \sum_i \frac{(\hbar\omega_i/k_B T)^2 \exp(\hbar\omega_i/k_B T)}{\left[\exp(\hbar\omega_i/k_B T) - 1\right]^2}, \quad (3.4)$$

respectively, where U_0 is the static lattice energy. The thermal expansion coefficient is given by [32]

$$\alpha(T) = \frac{1}{3B(T)} \sum_i \gamma_i C_{V,i}, \quad (3.5)$$

where $C_{V,i}$ is the summand in Eq. (3.4), and the Gruneisen parameter γ_i is defined as

$$\gamma_i = -\frac{\mathrm{d}(\ln \omega_i)}{\mathrm{d}(\ln V)}. \quad (3.6)$$

Results for these quantities will be shown below. In the case of a perfect crystal, one can also replace each sum over the $3N$ normal modes by a sum over wavevectors in reciprocal space. The latter representation is preferable at low temperatures because the first method neglects the low-frequency phonons associated with the long-wavelength modes, due to the finite size of the simulation cell. We have found that beyond 200 K the two methods yield essentially identical results.

3.2. Molecular dynamics and temperature scaling

The harmonic approximation is expected to be inadequate at high temperatures because it neglects phonon–phonon interactions. This problem can be overcome by using molecular dynamics.

Because molecular dynamics is based on classical mechanics, certain quantum corrections are necessary when comparing results with experiments at low temperatures. We have adopted the procedure whereby one defines a relation between the temperature of the simulation, T_{MD}, and the temperature of the experiment, T_{real}, by requiring that the internal energy of the simulation system be equal to that of the corresponding quantum system at T_{real} [33],

$$3(N-1)k_B T_{MD} = \frac{1}{2}\sum_i \hbar\omega_i + \sum_i \times \frac{\hbar\omega_i}{\left[\exp((\hbar\omega_i)/(k_B T_{real})) - 1\right]}, \quad (3.7)$$

wwhere ω_i is the ith normal mode frequency. The $(N-1)$ factor accounts for the fact that the center of mass is to be held fixed, and the sums are over the $3(N-1)$ non-zero frequencies. Another approach would be to estimate the correction terms in an expansion of the free energy in powers of Planck's constant [34,35]; this has been implemented in a study of structural and thermodynamic properties of an ionic crystal MgO [36].

The scaling relation between T_{MD} and T_{real} for the perfect crystal is shown in Fig. 2, where the phonon frequencies have been obtained from the force constants calculated from a static lattice at zero-pressure. Notice that $T_{real} = 0$ gives $T_{MD} = 510$ K, which can be considered as the zero-point temperature of our system. The relation Eq. (3.7) follows from the assumption that the internal energies of both the MD system and the real system behave harmonically, at least at low temperatures, where the scaling is important. We have reevaluated the force–constant matrix using the lattice parameter obtained from an MD simulation at constant (zero) stress and a temperature $T_{MD} = 510$ K. The resulting normal mode frequencies give a scaling factor which is effectively identical to that shown in Fig. 2, with a corresponding zero-point temperature of 507 K.

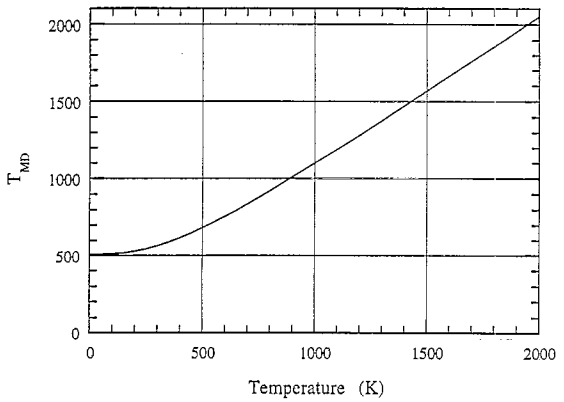

Fig. 2. Temperature scaling for SiC. Least squares polynomial fit gives: $T_{MD} = 513.45 - (0.18635)T_{real} + (0.0014644)T_{real}^2 - (9.8586 \times 10^{-7})T_{real}^3 + (3.4008 \times 10^{-10})T_{real}^4 - (4.6948 \times 10^{-14})T_{real}^5$.

The molecular dynamics determination of the thermal expansion coefficient and heat capacity is quite straight forward and follows from the expressions

$$\alpha = \frac{1}{a}\frac{da}{dT} \tag{3.8}$$

and

$$C_P = \left(\frac{\partial H}{\partial T}\right)_P, \tag{3.9}$$

where the enthalpy H is equal to the internal energy at zero pressure.

4. Thermal properties of single crystal β-SiC

Fig. 3 shows the thermal expansion coefficient calculated using both the harmonic approximation and molecular dynamics. In the former, Eq. (3.6) was evaluated by applying a linear fit to the appropriate phonon frequencies determined at three system volumes, V_0 and $(1 \pm 0.03)V_0$, where V_0 is the equilibrium volume at $T_{MD} = 0$ K. In the latter, the lattice parameter values found by simulation were fitted to a third-order polynomial.

Table 2
Gruneisen parameters

	Tersoff	Ab initio [39]	Experiment
TO(Γ)	1.16	1.07	1.02/1.102
LO(Γ)	1.16	1.02	1.01/1.091
TA(X)	0.40	0.12	
LA(X)	1.13	0.82	
TO(X)	1.31	1.46	1.30
LO(X)	1.13	1.16	
TA(L)	0.23	−0.13	−0.28
LA(L)	1.19	0.90	−0.11
TO(L)	1.25	1.31	1.24
LO(L)	1.10	1.15	1.30

As can be seen in Fig. 3, the harmonic approximation appears to yield values consistently closer to the experimental data [37,38] than does molecular dynamics. Such a result is not surprising at low temperatures, where there is uncertainty in our MD results because our scaling relation is necessarily flat (recall Fig. 2); however, it is certainly not expected at high temperatures. The fact that molecular dynamics yields greater expansivity at high temperatures compared to the harmonic approximation method seems reasonable on the grounds that the phonon–phonon interactions are ignored in the latter calculation. Our interpretation is that the apparent agreement between high-temperature data and the results from the harmonic approximation is fortuitous, and should be attributed to a cancellation of errors.

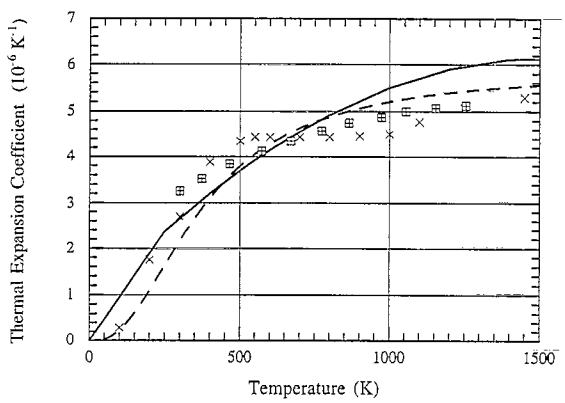

Fig. 3. Thermal expansion coefficient as a function of temperature, for the harmonic approximation (dashed line), MD values (solid line), experimental data [37] (crosses), and experimental data [38] (boxes with cross inside).

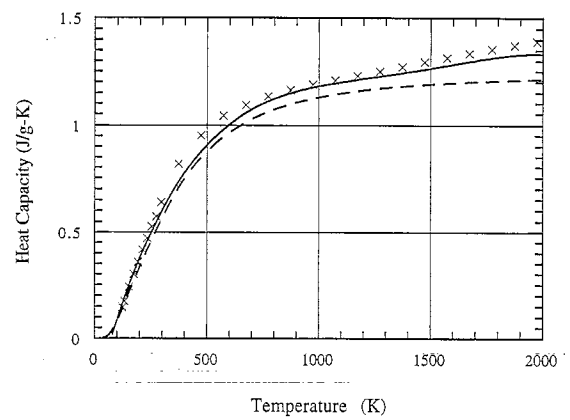

Fig. 4. Heat capacity as a function of temperature. Constant volume, C_V, is given by the dashed line, constant pressure, C_P, is given by the solid line, and experimental values for C_P [40] are given by the crosses.

It is seen from Eq. (3.5) that any potential which predicts well the Gruneisen parameters and the heat capacity will be successful in describing the thermal expansion. In Table 2 we show the calculated values of the Gruneisen parameters at the symmetry points Γ, X, and L obtained using the Tersoff potential and by ab initio methods [39], along with available experimental data [39]. While general agreement between Tersoff and ab initio seems satisfactory, the discrepancy in TA(L) is noteworthy. Also, both calculations yield significantly higher values for $\gamma_{\mathrm{LA}(L)}$ than experiment.

Fig. 4 shows the heat capacities at constant volume and pressure obtained using the Tersoff potential along with experimental data for C_p [40]. It is evident that this property is predicted well by the potential model. The agreement also serves to validate the temperature scaling relation that we have adopted in this work.

5. Conclusions

We have shown that using a current model description of interatomic forces in β-SiC, one can achieve a reasonably accurate prediction of the heat capacity and thermal expansion coefficient. Although neither property may seem particularly exciting from the standpoint of atomistic simulation, they are both nevertheless important physical properties from the standpoint of high-temperature materials applications. Knowledge of how well their temperature variations can be predicted should be useful as baseline information for studies of bimaterial interfaces, such as the calculation of thermal stresses.

Combined with our own experience in modeling Si [18] and C [41] with basically the same potential, we may conclude that the Tersoff description works well for covalent systems in which directional bonding effects are strong. Better results are indeed obtained for C and SiC than for Si [18,41]. We have also found that ionic interactions are clearly important in treating properly certain individual normal modes of vibration; on the other hand, their neglect seems to have little effect on integrated properties of the density of states. This is a rather general occurrence in materials modeling studies; namely, the robustness of a particular interatomic potential model can be quite property-specific.

As a compromise between computational efficiency and physical rigor, empirical many-body descriptions offer a reasonable starting point for an exploratory study. From the standpoint of theoretical connection to density functional theory, the basis of ab initio methods, the Tersoff model has been shown to emerge as a low-order variant of the bond-order potentials [42]. It is interesting that a connection between this model and an effective medium approximation developed for metals also has been noted [43].

The present results should provide a basis for the investigation of electronic-structure effects since ab initio calculations on SiC are now feasible [39,44,45]. Given the computational expense involved in these methods it would be appropriate to start with a description based on the tight binding approximation in which the band-structure contribution to the energy is treated through a model Hamiltonian. A self-consistent model has been developed [46]; even though its use thus far has been confined to structural properties at $T = 0$ only, it seems that temperature-dependent and vibrational properties soon can be treated in this way should the need arise.

In a follow-up paper, we extend our atomistic modeling approach to the calculation of thermal conductivity of SiC using the same Tersoff model. It will be shown that generally satisfactory agreement with experiment is attained for perfect as well as defective crystals. Furthermore, we will present results which suggest that while point defects have a negligible effect on the thermal expansion and heat capacity, they have a pronounced effect on the thermal conductivity; specifically, the conductivity is sharply reduced as a result of enhanced phonon scattering.

In closing, we note that atomistic simulation provides an effective approach to the fundamental understanding of thermal properties of crystalline solids, particularly in the presence of heterogeneities or extended defects. Nonuniform or nonequilibrium (driven) systems often have associated complex microstructures and kinetics which evolve over a hierarchy of length and time scales. Atomistic simulation, with molecular dynamics as a special case, needs to be integrated into a multiscale modeling scheme, along with mesoscopic techniques such as kinetic Monte Carlo, in order to effectively deal with the behavior of structural complexities in a thermal environment [47,48].

References

[1] R. Naslain, J. Lamon, D. Donmeingts, eds., High Temperature Ceramic Matrix Composites (Woodhead, Abington, Cambridge, UK, 1993).
[2] V. Heine, C. Cheng, G.E. Engel, R.J. Needs, in: Wide Band-Gap Semiconductors, MRS Symp. Proc., Vol. 242, ed. T.J. Moustakas, J.I. Pankove and T. Hamakawa (Materials Research Society, Pittsburgh, PA, 1992) and references therein.
[3] P. Rocco, H.W. Scholz, M. Zucchetti, J. Nucl. Mater. 191 (1992) 1474.
[4] M.C. Payne, M.P. Teter, D.C. Allen, T.A. Arias, D. Joannopoulos, Rev. Mod. Phys. 64 (1992) 1045.
[5] V. Vitek, D.J. Srolovitz, eds., Atomistic Simulation of Materials: Beyond Pair Potentials (Plenum, New York, 1989).
[6] A.P. Sutton, R.W. Balluffi, Interfaces in Crystalline Materials (Oxford University, Oxford, 1995) ch. 2; Interatomic Potentials for Atomistic Simulations, MRS Bull. 21 (Feb. 1996).

[7] C.Z. Wang, K.M. Ho, in: Advances in Chemical Physics, XCIII, ed. I. Prigogine and S.A. Rice (Wiley, New York, 1996).
[8] C.Z. Wang, K.M. Ho, C.T. Chan, Comput. Mater. Sci. 2 (1994) 93.
[9] J. Tersoff, Phys. Rev. B39 (1989) 5566.
[10] J. Tersoff, Phys. Rev. B37 (1988) 6991.
[11] J. Tersoff, Phys. Rev. Lett. 61 (1988) 2879.
[12] G.C. Abell, Phys. Rev. B31 (1985) 6184.
[13] H. Balamane, T. Halicioglu, W.A. Tiller, Phys. Rev. B46 (1992) 2250.
[14] K. Mizushima, S. Yip, E. Kaxiras, Phys. Rev. B50 (1994) 14952.
[15] S.J. Cook, P. Clancy, Phys. Rev. B47 (1993) 7686.
[16] P.J. Unger, T. Halicioglu, W.A. Tiller, Phys. Rev. B50 (1994) 7344.
[17] P.J. Unger, T. Takai, T. Halicioglu, W.A. Tiller, J. Vac. Sci. Technol. A11 (1993) 224.
[18] L.J. Porter, S. Yip, M. Yamaguchi, H. Kaburaki, M. Tang, J. Appl. Phys. 81 (1997) 96.
[19] F.H. Stillinger, T.A. Weber, Phys. Rev. B31 (1985) 5262.
[20] E. Pearson, T. Takai, T. Halicioglu, W.A. Tiller, J. Cryst. Growth 70 (1984) 33.
[21] M.I. Baskes, in: Computational Materials Modeling, ed. A. Noor and A. Needleman (ASME, New York, 1994) p. 23.
[22] M. Tang, S. Yip, J. Appl. Phys. 76 (1994) 2719.
[23] H. Huang, N.M. Ghoniem, J.K. Wong, M.I. Baskes, Modell. Sim. Mater. Sci. Eng. 3 (1995) 615.
[24] T. Halicioglu, Phys. Rev. B51 (1995) 7217.
[25] M. Tang, S. Yip, Phys. Rev. B52 (1995) 15150.
[26] M. Tang, S. Yip, Phys. Rev. Lett. 75 (1995) 2738.
[27] J. Tersoff, Phys. Rev. Lett. 64 (1990) 1757.
[28] J. Tersoff, Phys. Rev. B49 (1994) 16349.
[29] D.W. Feldman, J.H. Parker, W.J. Choyke, L. Patrick, Phys. Rev. 173 (1968) 787.
[30] D.W. Feldman, J.H. Parker, W.J. Choyke, L. Patrick, Phys. Rev. 170 (1968) 698.
[31] W.J. Choyke, D.R. Hamilton, L. Patrick, Phys. Rev. 133 (1964) A1163.
[32] N.W. Ashcroft, N.D. Mermin, Solid State Physics (Saunders College, Philadelphia, PA, 1976) ch. 25.
[33] C.Z. Wang, C.T. Chan, K.M. Ho, Phys. Rev. B42 (1990) 276.
[34] L.D. Landau, L.M. Lifshitz, Statistical Physics (Pergamon, London, 1958) ch. 33.
[35] J.-P. Hansen, J.J. Weis, Phys. Rev. 188 (1969) 314.
[36] M. Matsui, J. Chem. Phys. 91 (1989) 489.
[37] Z. Li, C. Bradt, J. Mater. Sci. 21 (1986) 4366.
[38] A. Taylor, R.M. Jones, in: Silicon Carbide, a High-Temperature Semiconductor, ed. J.R. O'Connor and J. Smiltens (Pergamon, Oxford, 1960) p. 147.
[39] C.-Z. Wang, R. Yu, H. Krakauer, Phys. Rev. B53 (1996) 5430.
[40] R.E. Taylor, H. Groot, J. Ferrier, Thermophysical Properties of CVD SiC, Thermophysical Properties Research Laboratory Report TPRL 1336, School of Mechanical Engineering, Purdue University, Nov. 1993.
[41] L.J. Porter, S. Yip, Atomistic Modeling of SiC Fiber Composites, Poster presentation at the AFOSR Ceramic Materials Program Review, Hueston Woods, OH, May 29–30, 1996.
[42] A.P. Horsfield, A.M. Bratkovsky, M. Fearn, D.G. Pettifor, M. Aoki, Phys. Rev. B53 (1996) 12694.
[43] D.W. Brenner, Phys. Rev. Lett. 63 (1989) 1022.
[44] K. Karch, P. Pavone, W. Windl, O. Schutt, D. Strauch, Phys. Rev. B50 (1994) 17054.
[45] B. Wenzien, P. Kackell, F. Bechstedt, Phys. Rev. B52 (1995) 10897.
[46] M. Kohyama, S. Kose, M. Kinoshita, R. Yamamoto, J. Phys.: Condens. Matter 2 (1990) 7791, 7809.
[47] G.R. Odette, J. Comput.-Aided Mater. Des. 3 (1996) 15.
[48] G. Martin, P. Bellon, F. Soisson, J. Comput.-Aided Mater. Des. 3 (1996) 187.